Bioorganic & Medicinal Chemistry Letters 19 (2009) 5511–5527

Contents lists available at ScienceDirect

Bioorganic & Medicinal Chemistry Letters

journal homepage: www.elsevier.com/locate/bmcl

# Bioorganic & Medicinal Chemistry Letters Vol. 19, No. 19, 2009

# Contents

## ARTICLES

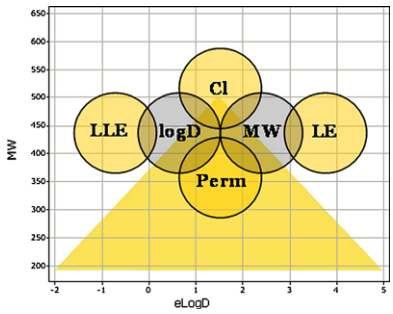




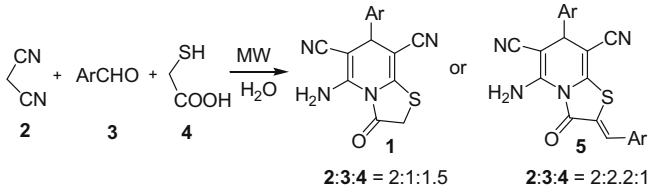


The green chemoselective synthesis of thiazolo[3,2-*a*]pyridines was achieved in water via microwave-assisted three-component reactions with different molar ratios of the reactants. Their antioxidant activity and cytotoxicity to carcinoma HCT-116 cells and mice lymphocytes were bioassayed. Compound **5d** suggested selective cytotoxicity to tumor cell line HCT-116 cells.



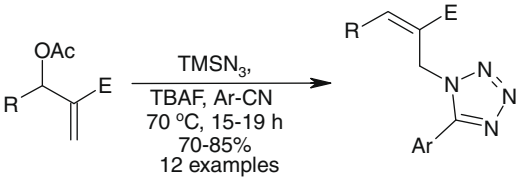




Replacing the galactose residue of CD22 ligand with benzyl or biphenylmethyl resulted in compounds with simplified structure and improved potency.

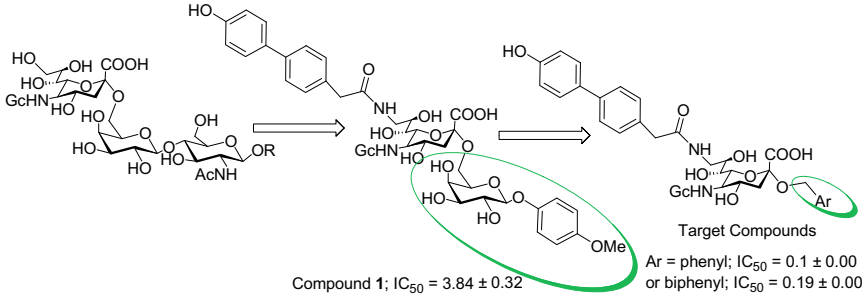

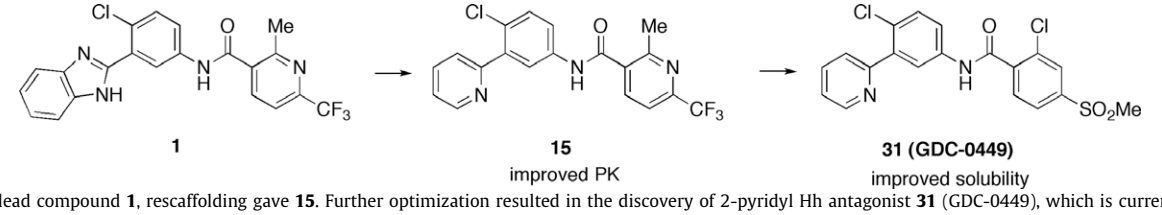


**1** **15** improved PK **31 (GDC-0449)** improved solubility

Starting from lead compound **1**, rescaffolding gave **15**. Further optimization resulted in the discovery of 2-pyridyl Hh antagonist **31** (GDC-0449), which is currently in human clinical trials.



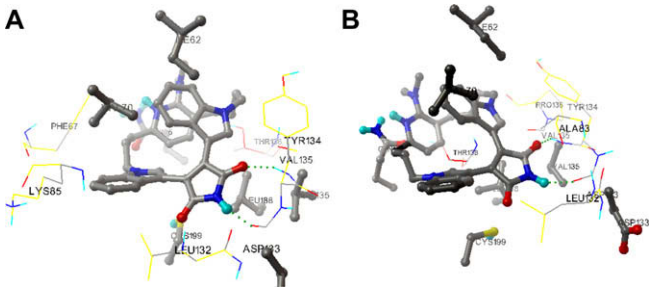


Interaction of Bis-(indole)maleimide pyridinophane (BIM) with (A) 1UV5 active site, (B) 2OW3 active site.



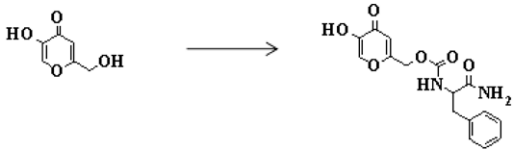


KA
$IC_{50}$ = 722.0 μM
$K_i$ = 582.7 μM

$KA\text{-}F\text{-}NH_2$
$IC_{50}$ = 14.7 μM
$K_i$ = 11.0 μM



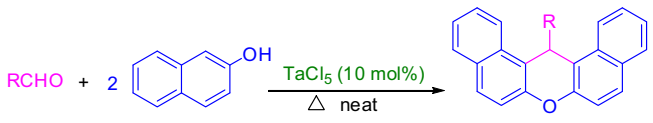


**1a-n** **2** **3a-n**

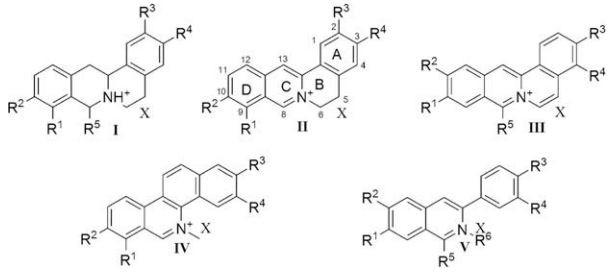



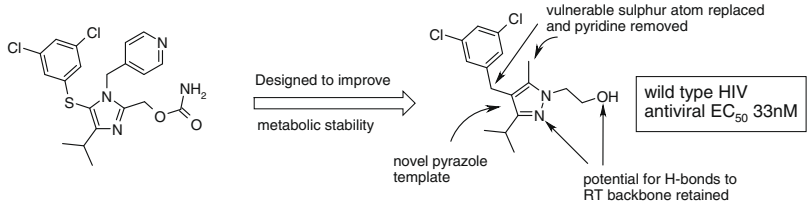


capravirine Design of prototype pyrazole inhibitor **6**

The design and synthesis of a novel series of non-nucleoside HIV reverse transcriptase inhibitors (NNRTIs) based on a pyrazole template is described. These compounds are active against wild type reverse transcriptase (RT) and retain activity against clinically important mutants.




**1**
wild type RT $IC_{50}$ 0.66μM
ligand efficiency (LE) 0.41
ligand-lipophilicity efficiency (LLE) 1.86

**52**
wild type RT $IC_{50}$ 0.35μM
ligand efficiency (LE) 0.43
ligand-lipophilicity efficiency (LLE) 3.77

Our efforts to reduce overall lipophilicity and increase ligand-lipophilicity efficiency (LLE) by modification of the 3- or 5-substituents of pyrazole **1**, a novel non-nucleoside HIV reverse transcriptase inhibitor (NNRTI) prototype were unsuccessful. In contrast replacement of the substituted benzyl group with corresponding phenylthio or phenoxy groups resulted in marked improvements in potency, ligand efficiency (LE) and LLE.



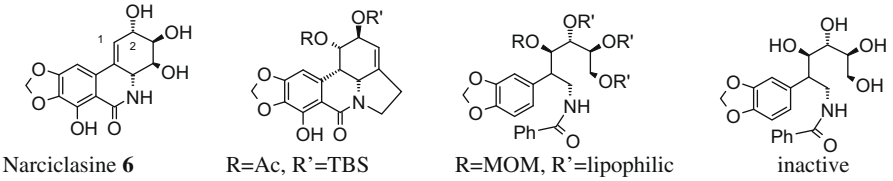

Narciclasine **6** R=Ac, R'=TBS R=MOM, R'=lipophilic inactive
*Ki* = 0.63 μM *Ki* = 0.21 μM *Ki* = 0.03 μM

The cytochrome P450 3A4 inhibitory activity of two fully synthetic series of *seco*-analogs of the lycorane-type anticancer amaryllidaceae alkaloids is presented. Potent inhibitors are identified and a comprehensive and consistent view of the P450 pharmacophore is revealed in this important series involving a double bond or small H-bond acceptor at the C1 position in conjunction with lipophilic substitution at C2, C3 and/or C4.

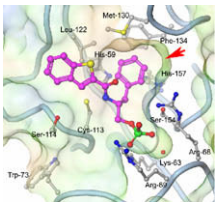


A series of novel non-peptide small molecular PIN1 inhibitors was discovered utilizing SBDD and combinatorial approach. The simplified pharmacophore opens the door for other drug-like Pin-1 inhibitor design.



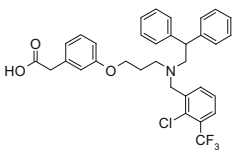


**2**; LXRα $EC_{50}$ = 200 nM

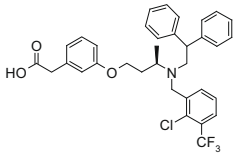


**14b**; LXRα $EC_{50}$ = 74 nM

SAR studies around *tertiary*-amine lead molecule **2**, an LXR full agonist, revealed that steric and conformational changes to the acetic acid and propanolamine groups produce dramatic effects on agonist efficacy and potency. The new analogs possess good functional activity, demonstrating the ability to upregulate LXR target genes, as well as promote cholesterol efflux in macrophages.



A series of rationally designed ROS1 tyrosine kinase inhibitors was synthesized and screened. Compound **12b** has showed good potency with $IC_{50}$ value of 209 nM, which is comparable with that of the reference lead compound **1**. Molecular modeling studies have been performed, that is, a homology model for ROS1 was built, and the screened inhibitors were docked into its major identified binding site. The docked poses along with the activity data have revealed a group of the essential features for activity. Overall, simplification of the lead compound **1** into compound **12b** kept the activity, while facilitated the synthetic advantages.

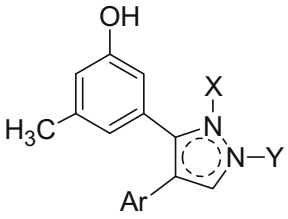


X = H, $CH_2CN$, Y = H, $CH_2CN$,
Ar = aryl, heteroaryl



Ac–Kψ[$CH_2NH$]LLLKLWLKLLK–$NH_2$

KL2

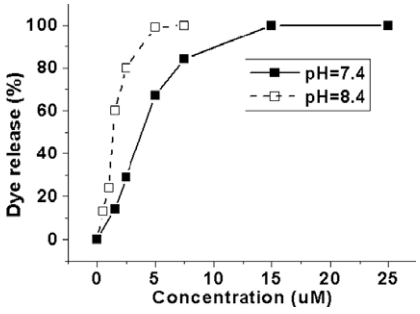

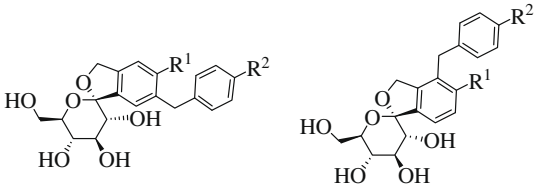


Two series of *O*-spiro *C*-aryl glucosides have been synthesized and evaluated for inhibition of hSGLT1 and hSGLT2.



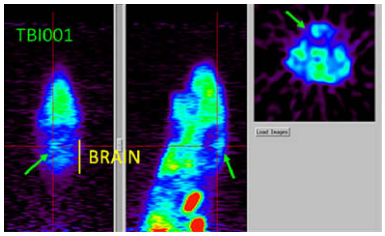


Fully automated synthesis and initial PET evaluation of a TSPO radioligand [$^{11}$C]PBR28 are reported.



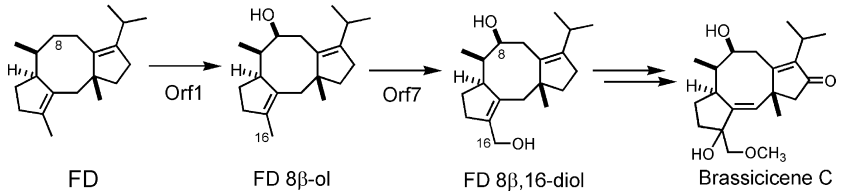


We revealed that the Orf1 was an 8β-hydroxylation enzyme to yield FD 8β-ol, followed by successive 16-hydroxylation by the Orf7 to produce FD 8β16-diol in the brassicicene C biosynthesis.



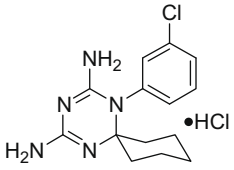


**4c**

[$^3$H]BTX, $IC_{50}$: 4.0 (0.5) μM

A series of 2,4-diamino-1,3,5-triazine derivatives was synthesized and examined as neuronal voltage-gated sodium channel blockers. Compound **4c** has shown significant in vitro neuronal sodium channel binding activity with no antifolate effect.

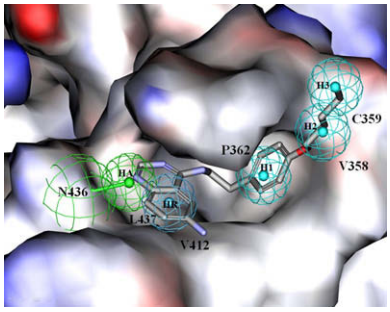


Pharmacophore features and a docking conformation are correctly matched onto NF-κB surface.



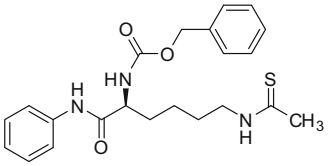

**1**

To identify cell-active sirtuin inhibitors containing *N*-thioacetyl lysine, we synthesized compound **1**, which was designed based on the structure of the reported *N*-ethoxycarbonylacetyl lysine-based sirtuin inhibitor NCS-12k. Compound **1** selectively inhibited SIRT1 in enzyme assays. Compound **1** also caused a dose-dependent increase in p53 acetylation in human colon cancer HCT116 cells, indicating the inhibition of SIRT1 in these cells.



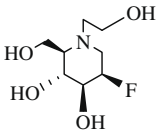

The synthesis of a monofluorinated α-glycosidase inhibitor from miglitol is reported.



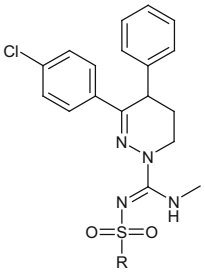

Tetrahydropyridazines represent a novel class of potent $CB_1$ receptor antagonists.

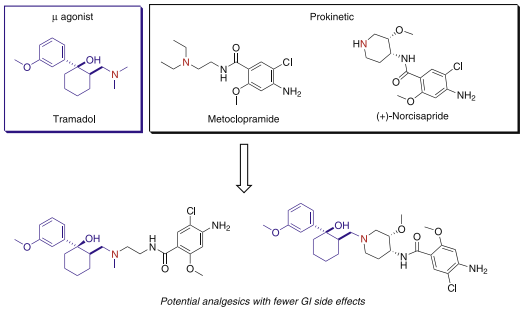




We have identified a series of diphenylmethylene hydroxamic acids as novel and selective HDAC class IIa inhibitors. *N*-Hydroxy-2,2-diphenylacetamide (**6**), has class IIa HDAC inhibitory activity in the sub-micromolar range, while the rigidified *N*-hydroxy-9*H*-xanthene-9-carboxamide (**13**), is slightly more selective for HDAC7. Substitution of **6** allows for the modulation of selectivity and potency amongst the class IIa HDAC isotypes.

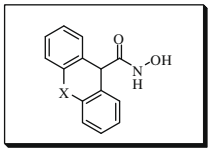

| cpd | X | HDAC class IIa isoforms $IC_{50}$ (μM) | | |
|---|---|---|---|---|
| | | 4 | 5 | 7 |
| **6** | H | 0.75 | 0.14 | 0.39 |
| **13** | O | 0.25 | 0.11 | 0.05 |



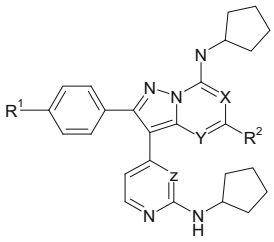

Synthesis of several pyrazolo[1,5-*c*]pyrimidines, pyrazolo[1,5-*a*]pyrimidines and pyrazolo[1,5-*a*][1,3,5]triazines with potent activity against herpes simplex viruses is described.



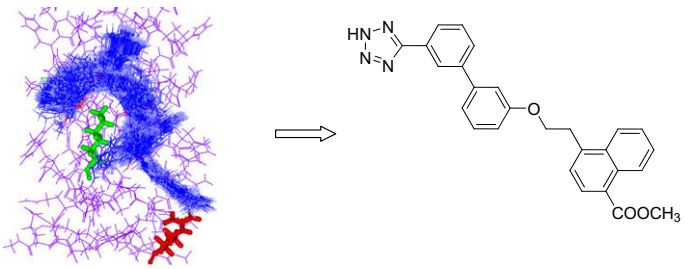

Structure-based design of small molecule ligands binding in the hydrophobic pocket of gp41 and blocking the helical bundle formation is described.

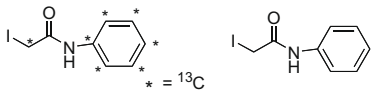


$^{13}C_7$-Labeled and unlabeled iodoacetanilide that covalently react with cysteine residues have been synthesized and applied to quantitative analysis of peptides and a protein.



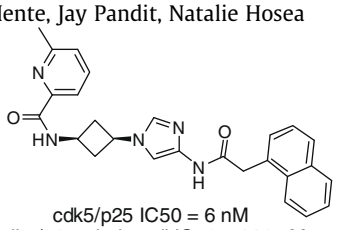


Using structure-based drug design, 4-aminoimidazoles were prepared with potent inhibition of cdk5/p25 in enzyme and whole cell assays and selectivity over cdk2.



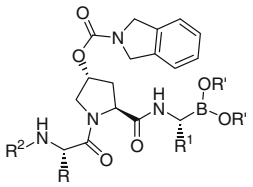

The synthesis and evaluation of a series of peptidomimetic boronic acid inhibitors of the HCV NS3/4A protease is described. Data on their biochemical and cellular activities, mutant protease activity, and genotype coverage is reported.



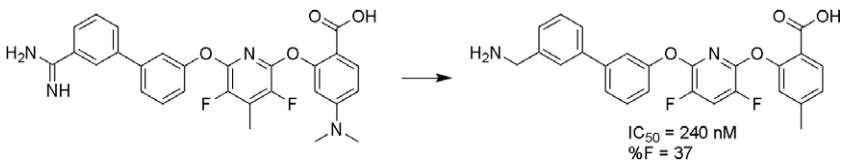


The discovery, synthesis, and early SAR work on a benzyl amine containing series of uPA inhibitors is reported.

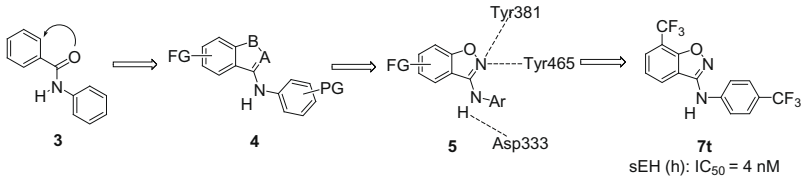


Distinct from previously reported urea and amide inhibitors of soluble epoxide hydrolase (sEH), a novel class of inhibitors were rationally designed based on the X-ray structure of this enzyme and known amide inhibitors. The structure–activity relationship (SAR) study was focused on improving the sEH inhibitory activity. Aminobenzisoxazoles emerged to be the optimal series, of which a potent human sEH inhibitor **7t** was identified with a good pharmacokinetics (PK) profile. The strategy of employing aminoheterocycles as amide replacements may represent a general approach to develop mimics of known hydrolase or protease inhibitors containing an amide moiety.



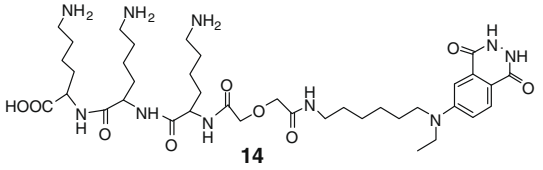


Rapid assays for bacteria have been developed utilizing novel LysLysLys-isoluminol (**14**) and GluGlu-isoluminol (**16**) probes. Compared to two conventional methods that are widely used, namely nucleic acid probes and polymerase chain reaction (PCR) assays, these current probe assays may have certain advantages, such as high sensitivity, and short preparation and assay time.



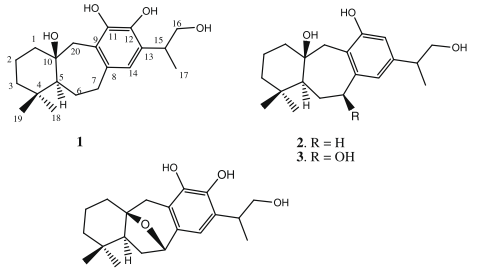


Bioactivity-guided column chromatographic separation of hexane extract led to the isolation of four new cytotoxic icetexane diterpenes (**1**–**4**), along with five known compounds (**5**–**9**). Compounds **1**–**3** were tested against the cancer cell lines for their cytotoxicity.



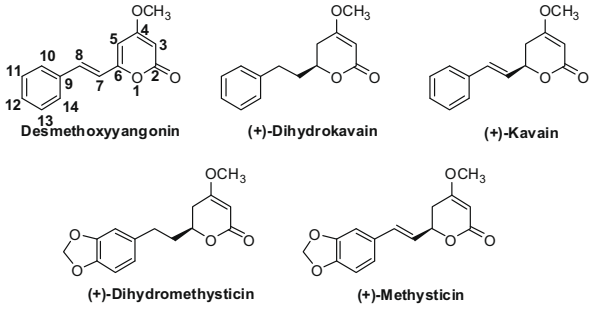

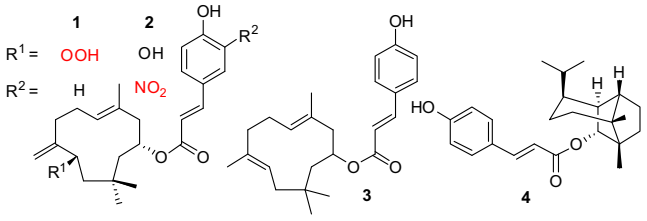


Three new humulane-type sesquiterpenes **1**–**3**, and a copaborneol derivative **4** were isolated from the methanol extract of *Pilea cavaleriei* subsp. *crenata*. Their structures were elucidated and cytotoxic activities were evaluated.



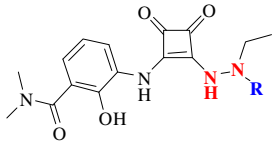


**Wherein R = H, alkyl, acyl, aryl, heteroaryl, etc**

A novel series of 3-amino-4-hydrazine-cyclobut-3-ene-1,2-diones as potent and selective CXCR2 chemokine receptor antagonists were identified.



Through iterative design cycles we have discovered a number of novel new classes where the imidazo[1,5-*a*][1,2,4]-triazolo[1,5-*d*][1,4]benzodiazepine was deemed the most promising $GABA_A$ α5 inverse agonist class with potential for cognitive enhancement. This class combines a modest subtype binding selectivity with inverse agonism and has the most favourable molecular properties for further lead optimisation towards a central nervous system (CNS) acting medicine.

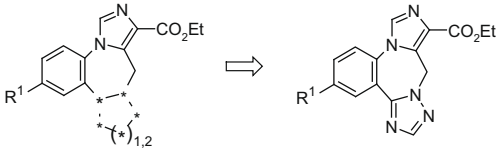




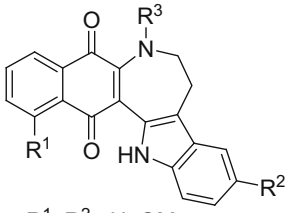


$R^1$, $R^2$= H, OMe
$R^3$= H, $CH_3$, $C_3H_7$, Allyl, Bn

The synthesis and inhibitory effects on pro-inflammatory cytokines of 1,5,6,7,8,14b-hexahydro-naphtho[2,3-*d*]-azepino[4,5-*b*]indole-9,14-diones are reported.

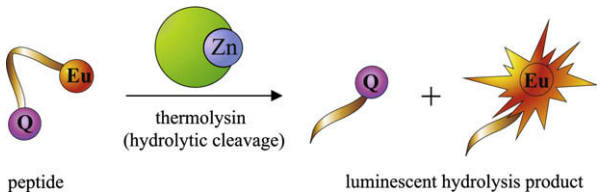


A new fluorogenic, lanthanide-based oligopeptide substrate for the detection of the zinc-dependent endoprotease thermolysin is described. Using time-resolved fluorescence measurement, a highly sensitive assay for thermolysin was developed with a 50 pM detection limit (3.5 fmol).



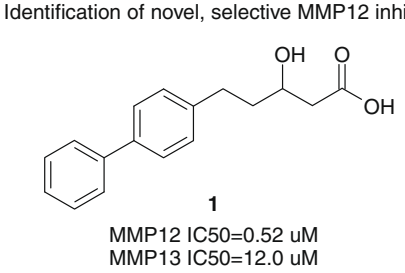




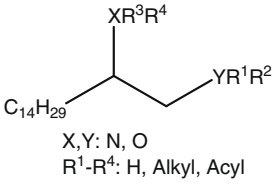


A number of dihydrosphingosine analogues were tested in vitro against several strains of *Mycobacterium tuberculosis* (*MTB*). Three (**3**, **4b** and **8b**) out of the fifteen evaluated compounds, displayed MIC values of 1.25 μg/mL on virulent H37Rv and several MDR strains and, more interestingly, on one clinical isolate resistant to all the first-line anti-TB drugs.



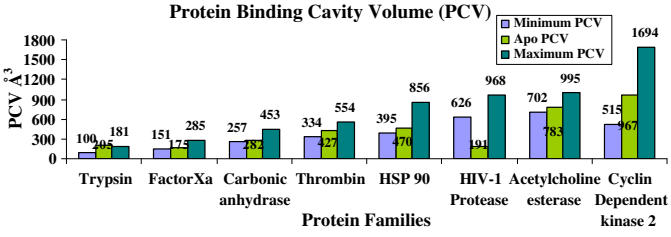


Variation in protein binding cavity volume (PCV) for different ligands illustrated in the graph for eight different protein families encompassing 200 protein–ligand complexes.

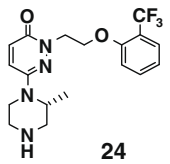


**24**

The design, synthesis and biological activity of pyridazinone derived, selective 5-HT$_{2C}$ agonists is described. Compound **24** showed efficacy in a pre-clinical model of urethral function which highlights potential efficacy in stress urinary incontinence.



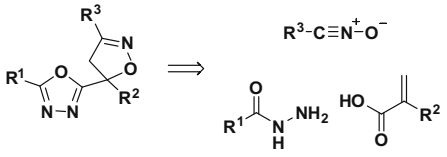




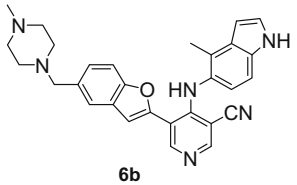


**6b**

Analog **6b** with a 4-methylindol-5-ylamino group at C-4 and a 5-[(4-methylpiperazin-1-yl)methyl]-1- benzofuran-2-yl group at C-5 had an IC$_{50}$ value of 0.28 nM for the inhibition of PKCθ.



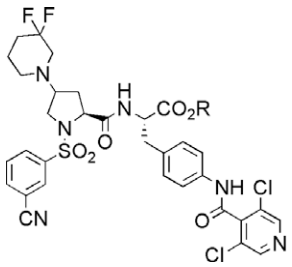


**R = H (MK-0617):**
IC$_{90}$ ( human whole blood): 0.2 nM
**R = Et:**
Receptor occupancy at 12 h post dose:
80% (5 mg/kg po)

## OTHER CONTENTS



*Corresponding author

ⓘ+ Supplementary data available via ScienceDirect

## COVER

Overlay of high resolution co-crystal structures of *R*-**22**-ADP (cyan) and **1**-ADP (green) bound in an allosteric binding site of the mitotic kinesin KSP. [Roecker, A. J.; Coleman, P. J.; Mercer, S. P.; Schreier, J. D.; Buser, C. A.; Walsh, E. S.; Hamilton, K.; Lobell, R. B.; Tao, W.; Diehl, R. E.; South, V. J.; Davide, J. P.; Kohl, N. E.; Yan, Y.; Kuo, L. C.; Li, C.; Fernandez-Metzler, C.; Mahan, E. A.; Prueksaritanont, T.; Hartman, G. D. *Bioorg. Med. Chem. Lett.* **2007**, *17*, 5677.]

Indexed/Abstracted in: Beilstein, Biochemistry & Biophysics Citation Index, CANCERLIT, Chemical Abstracts, Chemistry Citation Index, Current Awareness in Biological Sciences/BIOBASE, Current Contents: Life Sciences, EMBASE/Excerpta Medica, MEDLINE, PASCAL, Research Alert, Science Citation Index, SciSearch, TOXFILE

ELSEVIER

ISSN 0960-894X